Rend. Fis. Acc. Lincei (2013) 24:163–176
DOI 10.1007/s12210-013-0239-z

Evidence for deep subduction of Austroalpine crust (Texel Complex, NE Italy)

Stefano Zanchetta · Stefano Poli · Daniela Rubatto · Andrea Zanchi · Giovanni Maria Bove

Received: 16 February 2013 / Accepted: 16 April 2013 / Published online: 1 May 2013

Abstract We report here the discovery of UHP eclogites in the Ulfas Valley within the Texel Complex (Meran, NE Italy), which has important implications on the evolution of the Austroalpine nappe stack in the Eastern Alps. Exsolved K-feldspar and phengite lamellae within omphacite relics, together with an unusually high K-content of the host clinopyroxene, point to equilibrium pressures at least close to the quartz/coesite transition. The age of the high-pressure metamorphism is constrained by U–Pb dating of metamorphic zircon at 85 ± 4 Ma. These new data suggest pressure conditions for the Cretaceous eclogitic metamorphism of the Texel Complex higher than hitherto reported data, possibly indicating that several sectors of the Africa-Adria derived Austroalpine margin were subducted to mantle depths during the early stages of the Alpine orogeny.

Keywords Austroalpine · UHP metamorphism · K-feldspar exsolutions · Cretaceous subduction

Electronic supplementary material The online version of this article (doi:10.1007/s12210-013-0239-z) contains supplementary material, which is available to authorized users.

S. Zanchetta (✉) · A. Zanchi
Dipartimento di Scienze Geologiche e Geotecnologie, Università degli Studi di Milano Bicocca, Piazza della Scienza 4, 20126 Milan, Italy
e-mail: stefano.zanchetta@unimib.it

S. Poli
Dipartimento di Scienze della Terra, Università degli Studi di Milano, Via Botticelli, 20133 Milan, Italy

D. Rubatto
Research School of Earth Sciences, The Australian National University, Canberra, ACT 0200, Australia

G. M. Bove
Ufficio Geologia e Prove Materiali, Provincia Autonoma di Bolzano, Via Val d'Ega 48, Cardano, Italy

1 Introduction

Ultra High Pressure (UHP) rocks and eclogites represent first-order constraints for the interpretation of the geodynamic evolution of collisional orogens (Chopin 2003). As such, they are important geological markers. Subduction of continental crust to depths of more than ~90 km, i.e. above the quartz/coesite transition, is limited in the Alps to the Dora Maira (Chopin 1984) and the Zermatt-Saas (Reinecke 1991) units of the Western Alps and to the garnet peridotite lenses within the Adula-Cima Lunga unit of the Central Alps (Heinrich 1986) (Fig. 1). In the Eastern Alps, eclogites equilibrated at more than 2 GPa are reported from the Koralpe/Saualpe unit and from the Pohorje Mountain (Miller and Konzett 2005b; Janák et al. 2004, 2006).

Other than the above mentioned UHP rocks, several other eclogite occurrences, equilibrated at lower pressures, are reported from the Eastern Alps. All together they form the Koralpe-Wölz unit (Schimd et al. 2004, 2008; Handy et al. 2010) that extends from the Texel and Schneeberg complexes in the west, to the Pohorje Mountains in the east (Fig. 1). Available geochronological data constrain the age of the high-pressure metamorphism of the Koralpe-Wölz unit to the Late Cretaceous (Thöni 2006), with data obtained from high-retentively isotopic system (e.g. U–Pb, Sm–Nd and Lu–Hf) that give a shorter time span for peak pressures at ca. 95–80 Ma (Habler et al. 2006; Thöni et al. 2008; Miller et al. 2005c).

With the only noticeable exception of the Koralpe/Saualpe eclogites (Miller et al. 2005a) and the peridotite

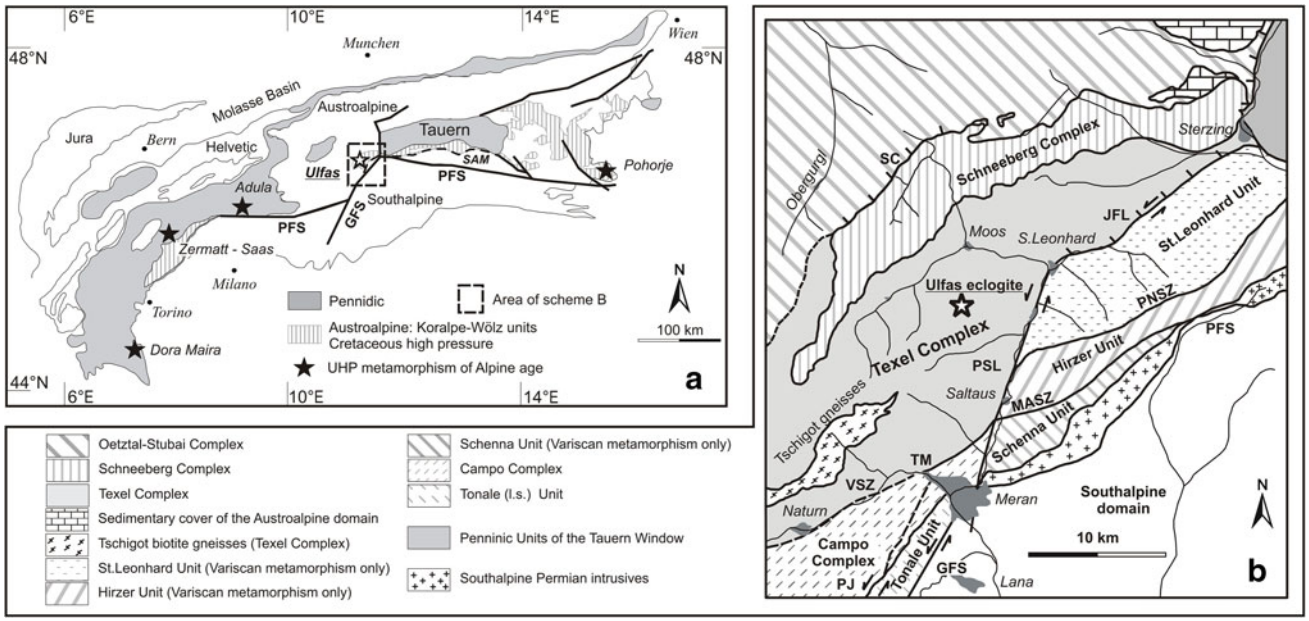

Fig. 1 **a** Simplified tectonic scheme of the Alps with ultrahigh-pressure rocks of Alpine age. **b** Geological outline of the Austroalpine basement in the western Eastern Alps, modified from Bargossi et al. (2010). *SC* Schneeberg normal fault, *PNSZ* Pennes shear zone, *MASZ* Masul Shear Zone, *PL* Periadriatic lineament, *VSZ* Vinschgau Shear Zone, *PJ* Pejo line, *GD* Giudicarie line, *TM* Thurnstein mylonites, *JF* Jaufen line, *PS* Passeier line

lenses in the Pohorje Mountain unit (Janák et al. 2004, 2006; Miller et al. 2005b; Thöni et al. 2008), for which peak pressures of 2–2.4 GPa and >2.1 GPa were respectively suggested, all the other eclogites of the Koralpe-Wölz unit, equilibrated at lower pressure, just above the garnet amphibolite facies.

Here we describe the occurrence of eclogites within the Texel Complex, which possibly recorded UHP conditions. The timing of eclogitic metamorphism is constrained by U–Pb dating of metamorphic zircons. Our new data provide further constraints for the geodynamic evolution of the high-pressure Austroalpine units of the Eastern Alps.

2 Geological setting

The Austroalpine basement of the Eastern Alps, west of the Tauern Window includes several units with different and diachronous tectonometamorphic evolution. Its southern part extends between the Schneeberg Complex (Sölva et al. 2005) to the north and the Periadriatic Lineament to the south (Fig. 1). The Tertiary Passeier and Jaufen Lines are part of a major fault-system (SAM, Southern limit of Alpine Metamorphism, Hoinkes et al. 1999; Viola et al. 2001) that separates tectonic units with pre-Alpine metamorphism to the south-east (units in Fig. 1b) from units with a significant Alpine overprint to the north-west, like the Schneeberg and the Texel units (Spiess 1995).

The Texel Complex displays a polymetamorphic evolution with a dominant amphibolite facies overprint of Alpine age (Hoinkes et al. 1999; Sölva et al. 2005 and ref. incl.). It is bounded by the Schneeberg Complex to the north, the Passeier and Jaufen lines to the east (Viola et al. 2001) and the Vinschgau Shear Zone (VSZ: Schmid and Haas 1989) to the south. Field structural analysis and petrological studies (Zanchetta 2010; Bargossi et al. 2010) indicate that the Texel and the Schneeberg complexes experienced a common tectonometamorphic evolution since the deformation stage (D_2 in Bargossi et al. 2010) that accompanied the regional amphibolite facies metamorphism.

The Texel complex consists of garnet–staurolite–kyanite mica schists and gneisses with minor amphibolites and marbles (Bargossi et al. 2010). Eclogites are preserved as small boudins within garnet amphibolites in several localities, e.g. Saltaus (Hoinkes et al. 1991; Habler et al. 2006), Moos (Poli 1991) S. Martin (Bargossi et al. 2010) and Ulfas. In addition, garnet amphibolites containing diopside + plagioclase ± amphibole symplectites are widespread throughout the complex. Hoinkes et al. (1991) reported minimum pressures of 1.1–1.2 GPa at 500–550 °C; higher temperatures were suggested by Spalla (1993) and Poli (1991), respectively reaching 640–680 °C and 700 °C. Recent garnet Sm–Nd data (Habler et al. 2006) constrain eclogite facies metamorphism at 85 ± 5 Ma.

3 Samples description

The partly amphibolitized eclogites crop out along the north-western slope of the Ulfas Valley (46°47′20.09″N, 11°9″49.95′E), about 15 km N of Meran (Fig. 1b). The eclogites are preserved as metric to decametric light-coloured boudins (Fig. 2) within layered amphibolites, with carbonates and biotite bearing levels, which form large lenses enclosed in garnet–kyanite–staurolite mica schists and gneisses (Fig. 2a, b).

The compositional layering of the garnet amphibolites (alternated amphibole–plagioclase and amphibole–garnet layers) is subparallel to the regional amphibolite facies foliation, S_2, in surrounding gneisses and mica schists (Zanchetta 2006, 2007; Bargossi et al. 2010).

The contact between the partly amphibolitized eclogites and the garnet amphibolites is gradational and it is over a few centimetres (Fig. 2d). The eclogites are medium to coarse grained with inequigranular texture. Garnet porphyroblasts reach 1.5 cm in diameter. The grain size of mineral phases forming the high-pressure assemblage is found to decrease from the core towards the rim of the boudins (see Fig. 2d), probably as an effect of retrogression. The banded texture, made of alternating garnet–zoisite–amphibole rich level and light-green clinopyroxene-rich levels is evident on the Ulfas outcrop (Fig. 2b, c). Green amphibole–plagioclase coronae around garnet porphyroblasts are common and well recognizable also in hand specimen.

Samples used for petrology and zircon dating (GB1396B, GB1396C, GB13241G) come from the metric boudin (Fig. 2b) at the right-bottom corner of the map in Fig. 2a.

4 Analytical methods

4.1 Mineral chemistry and whole rock data

Quantitative chemical analyses of mineral phases were obtained with an ARL SEMQ and JEOL 8200 Superprobe, both equipped with WDS spectrometers, at the University of Milan. Operating conditions were 15 kV and 15 nA of beam current. Natural silicates have been used as standards and resulting data were processed through a ZAF correction procedure. All the analyses were collected using a focussed beam, except for micas for which a 5 μm probe diameter was adopted. Textural characteristics of studied samples, determined through optical microscope observations, were checked by SEM analyses.

Representative chemical data of garnet, omphacite and phengite of the eclogite facies phase assemblage are reported in Table ESM1 (online resource 1), Table ESM2 (online resource 2) and Table ESM3 (online resource 3),

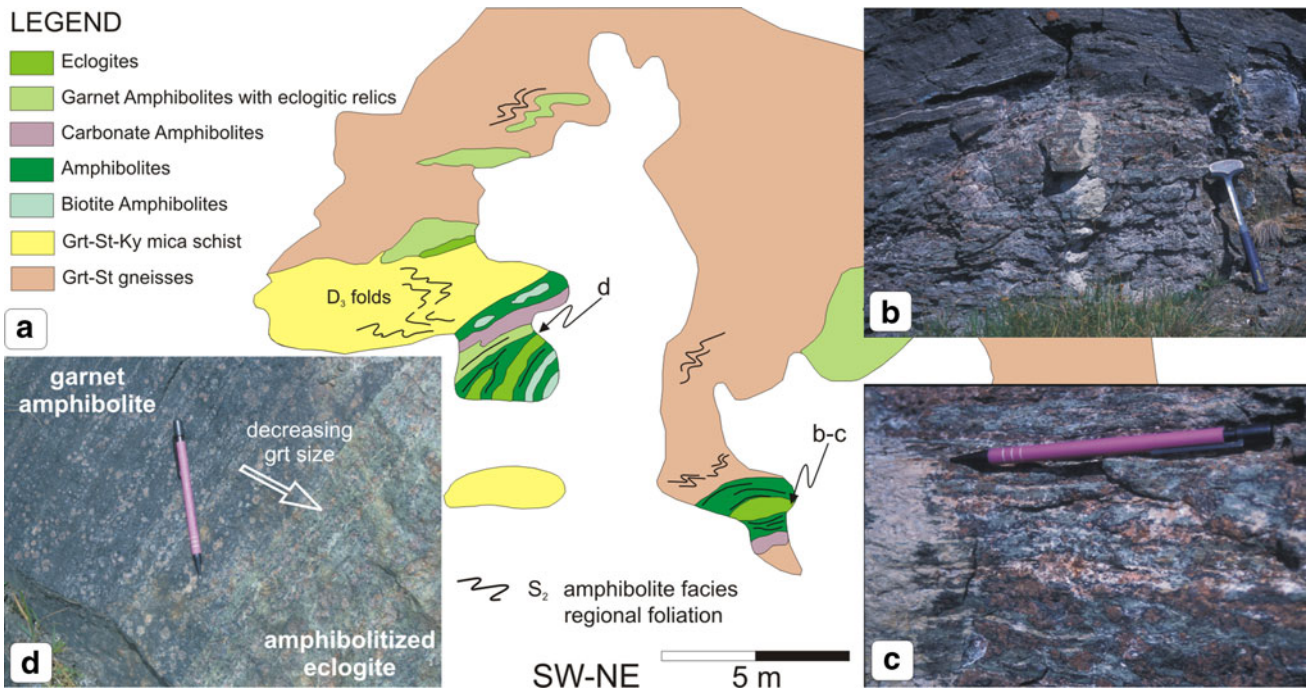

Fig. 2 **a** Sketch of the Ulfas eclogites main outcrop. **b** Metre-sized eclogite boudin within garnet amphibolites. **c** Textural aspect of the eclogites with well-developed mineralogical layering. **d** Gradual eclogite–amphibolite transition at the boudin boundary, note the progressive grain size reduction of garnet porphyroblasts from *right* to *left* of the image

respectively. In Table ESM4 (online resource 4) and Table ESM5 (online resource 5) microprobe analyses of, respectively, K-feldspar and phengite exsolution lamellae are reported. Mineral abbreviations are as per Kretz (1983).

Analyses for bulk rock major, minor and trace elements were determined at the ACME Analytical Laboratories Ltd. in Vancouver (Canada). Total abundances of the major oxides were obtained by ICP-ES (Inductively Coupled Plasma Emission Spectroscopy) following a $LiBO_2$ fusion and dilute nitric digestion. The REE and the refractory elements were determined by ICP-MS (Mass Spectroscopy) following $LiBO_2$ fusion and dilute nitric digestion. The precious and base metals were digested in *acquaregia* and then analyzed by ICP-MS. Obtained bulk rock compositions are reported in Table ESM6 (online resource 6).

4.2 SHRIMP U–Pb geochronology

Zircons for trace elements and U–Th–Pb analysis were prepared as mineral separates mounted in epoxy and polished down to expose the grain centres. Cathodoluminescence (CL) investigation of zircon was carried out at the Electron Microscope Unit, Australian National University, with an HITACHI S2250-N scanning electron microscope working at 15 kV, ~60 μA and ~20 mm working distance.

Trace element analyses were performed by Laser Ablation—ICP-MS at the Research School of Earth Sciences (RSES) using a pulsed 193 nm ArF Excimer laser with 100 mJ energy at a repetition rate of 5 Hz (Eggins et al. 1998) coupled to an Agilent 7,500 quadrupole ICP-MS. Spot size varied between 54 and 86 μm in diameter. External calibration was performed relative to NIST 612 glass. Internal standard was Si, according to stoichiometry (32.45 wt% SiO_2). Accuracy of the analyses was evaluated with a BCR-2G secondary glass standard and is generally better than 15 %.

U–Pb analyses were performed using a sensitive, high-resolution ion microprobe (SHRIMP II) at the RSES. Instrumental conditions and data acquisition for zircon analysis were generally as described by Williams (1998). The data were collected in sets of six scans throughout the masses. The measured $^{206}Pb/^{238}U$ ratio was corrected using reference zircons from Temora (Black et al. 2003). A zircon of known composition (SL 13) has been used to determine the U content of zircon. The data were corrected for common Pb on the basis of the measured $^{207}Pb/^{206}Pb$ ratios as described in Williams (1998) and assuming the composition predicted by the Stacey and Kramers model (1975). Age calculations were done using the software Isoplot/Ex (Ludwig 2000).

SHRIMP U–Th–Pb analyses are reported in Table ESM7 (online resource 7). REE contents in zircons determined by ICP-MS are reported in Table ESM8 (online resource 8).

5 Petrology

The Ulfas eclogites have a complex mineralogy made of clinopyroxene, garnet, amphibole, zoisite/clinozoisite, epidote, calcite, titanite, phengite, K-feldspar, ilmenite, rutile, chlorite, quartz, apatite and zircon.

The absence of internal deformation in the boudins and the strong recrystallization under amphibolite facies conditions made difficult the reconstruction of equilibrium phase assemblages from the pre-eclogite to the latest stage of exhumation. At the thin section scale, the Ulfas eclogites appear substantially undeformed. A compositional layering made by alternating garnet–amphibole–zoisite and symplectitic clinopyroxene–plagioclase layers (Fig. 3a–d) represents the main microstructures in the analyzed samples. Within single layers no preferred orientation of eclogitic mineral has been observed.

The garnet porphyroblasts are up to 2 cm in diameter and consist of three different textural and compositional zones (Fig. 4a, b). Garnet cores (grt_I) contain inclusion of amphibole, epidote, ilmenite, rutile and apatite. In some samples an internal foliation (S_i) is individuated by trails of micrometric ilmenite and quartz crystals. The foliation is disposed at high angle with the grt_I–grt_{II} boundary and it terminates abruptly 3–5 mm from the porphyroblasts centre. Grt_I cores ($Grs_{31}Pyr_{11}Alm_{57}Sps_1$) are interpreted as pre-eclogitic (M0 phase assemblage) as they lack inclusions of high-pressure minerals.

A second generation of garnet (grt_{II}) grows as idiomorphic rims around grt_I cores. Grt_{II} constitutes volumetrically the major part of garnet porphyroblasts. This eclogite facies assemblage (M1 phase assemblage) consists of grt_{II} ($Grs_{22}Pyr_{10}Alm_{67}Sps_1$) (Fig. 4a), omphacite ($cpx_I$: $Jd_{45–48}$, Fig. 5), phengite (phn_I with 3.54–3.60 Si a.p.f.u., Fig. 6), zoisite (2.8–2.95 Al a.p.f.u.) (Fig. 3e), Al-rich titanite (ttn_I with X_{Al} up to 0.34, where $X_{Al} = Al/Al + Fe^{3+} + Ti$, Fig. 7) and calcite. Titanite substitutes rutile as the Ti-bearing phase (Fig. 3f).

At a later stage, the eclogitic assemblage was partly substituted by a second generation of clinopyroxene (cpx_{II}, with up to Jd_{10}) and pargasitic amphibole symplectites, phengite rims with lower Si-content (3.40–3.45 a.p.f.u.) on existing phengite, and Al-poor titanite, (M2, ttn_{II} with X_{Al} 0.05–0.08).

The successive evolution stages took place at lower pressure, well within the amphibolite facies, with the development of Na-free diopside (cpx_{II}) + plagioclase and amphibole + plagioclase symplectites on former eclogitic clinopyroxenes (M3). During this retrogression stage

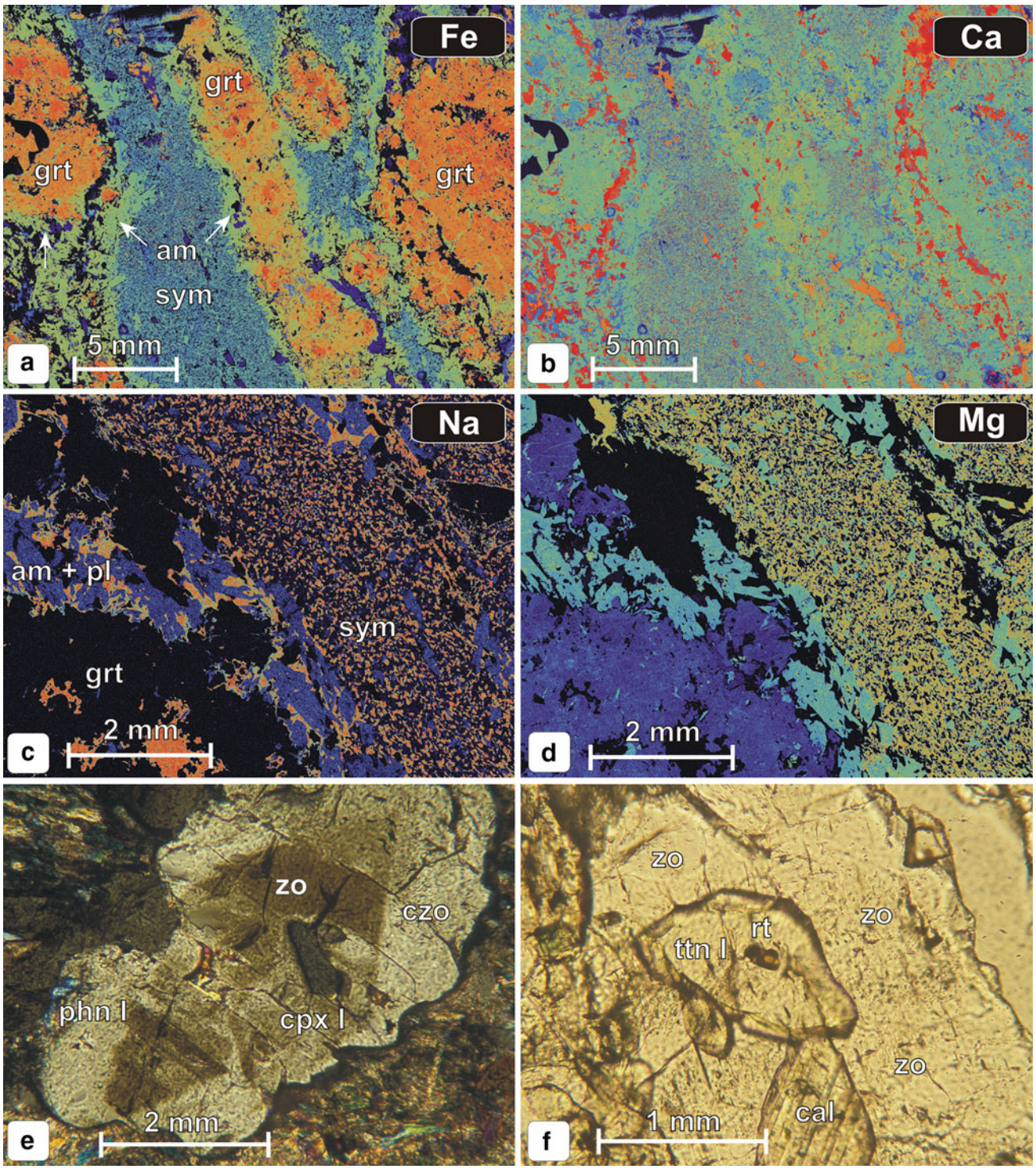

Fig. 3 Major element X-ray maps of Ulfas eclogite are represented in Fig. **a–d** at different scales and for different elements. *Warm colours* indicate higher concentrations, and *cool colours* indicate lower concentrations. *Am* amphibole, *cal* calcite, *cpx* clinopyroxene, *czo* clinozoisite, *grt* garnet, *phn* phengite, *pl* plagioclase, *rt* rutile, *sym* symplectitic matrix, *ttn* titanite, *zo* zoisite. **e** Clinozoisite overgrows on zoisite containing inclusion of cpx I. **f** Rutile relict within Al-rich titanite (ttn I) stable within the eclogitic facies phase assemblage

garnet porphyroblasts are subjected to irregular resorption and occasionally growth of a thin Ca-rich rim (grt_{III}, Fig. 4) with a $Grs_{26}Pyr_{11}Alm_{62}Sps_1$ mean composition.

The latest exhumation stages are recorded by substitution of garnet rims (grt_{III}) by Fe-pargasitic hornblende + plagioclase (An_{15}) coronae (M4). Finally, during decompression,

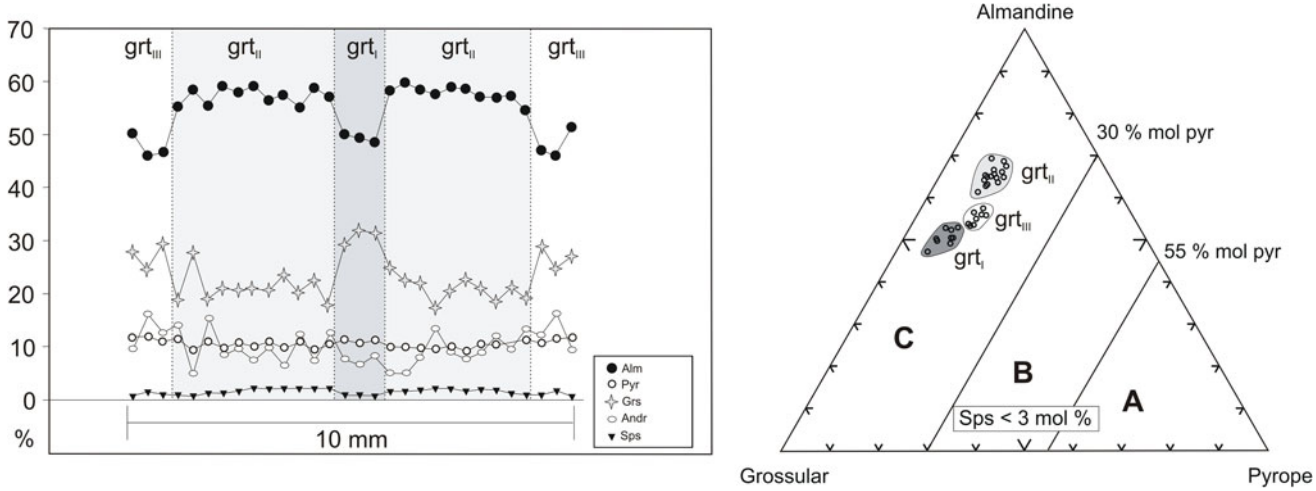

Fig. 4 **a** Compositional profile of garnet. The eclogite facies relics are preserved in the garnet-II zone, whereas garnet cores (zone I) are almost inclusion-free, except for tiny rutile crystals. **b** Composition of Ulfas garnets plotted in the eclogitic garnet classification of Coleman et al. (1965). They plot within the Alpine-type eclogites (field C)

epidote, albite and minor chlorite formed along veins throughout the rock (Fig. 2b).

5.1 Possible UHP relics

The phase assemblage of the higher pressure stage (M1) shows remarkable differences with respect to the other eclogites of the Texel Complex (Hoinkes et al. 1991; Habler et al. 2006).

1. The maximum Si-content in the matrix phengites of the Ulfas eclogites is significantly higher (3.61 versus 3.40 a.p.f.u., Habler et al. 2006).
2. Unusually high K-contents up to 0.09 K_2O wt% have been measured in Na-clinopyroxene (cpx_I).
3. K-feldspar and phengite lamellae of 10–30 μm in size are present in several samples within the omphacite relics (Fig. 8a, b). The lamellae are homogeneously distributed and aligned parallel to the (010) of the host clinopyroxene. The orientation and spatial distribution of the lamellae support the exsolved nature of K-feldspar and phengite from a previous Si-rich and K-rich clinopyroxene. The oligoclase patches that are occasionally found near K-feldspar, together with phengite exsolutions (Fig. 8a, b), are interpreted as the eclogite to amphibolite facies decompressional stage with omphacitic clinopyroxene progressively transformed into diopside + amphibole + plagioclase symplectites.

5.2 Thermobarometry and P–T path

Minimum P–T conditions for the Ulfas eclogites were calculated using conventional geothermobarometers. Additional constraints come from experimental data on H_2O-saturated MORB-like systems (Schmidt and Poli 1998; Poli and Schmidt 2004). The P–T estimates of the eclogite facies assemblage (M1) were obtained with the garnet–phengite (Green and Helmann 1982) and garnet–clinopyroxene (Krogh Ravna 2000) thermometers, and the garnet–phengite–clinopyroxene barometer (Waters and Martins 1996; Krogh Ravna and Terry 2004). Resulting P–T of equilibrium for the pressure peak phase assemblage was 2.65–2.90 GPa and 630–690 °C with estimated errors of ±0.20 GPa and ±50 °C (Fig. 9). The formation of Na-diopside (Jd_{10}) and pargasite after omphacite and the decreasing Si-content of phengite rims (3.40 p.f.u.) indicate progressive re-equilibration of the pressure peak paragenesis close to the eclogite–amphibolite facies boundary.

The full, amphibolite facies re-equilibration (M4), corresponding to the formation of amphibole-plagioclase coronae around garnet, took place at 610–650 °C and 0.9–1.1 GPa, according to the geothermobarometers of Holland and Blundy (1994) and Dale et al. (2000).

The resulting P–T path of the Ulfas eclogites (Fig. 9) is clockwise, with decompression from the eclogitic peak to the amphibolite facies re-equilibration accompanied by minor cooling.

6 Zircon age and composition

In thin section, zircons were observed as inclusion in the garnet and within the symplectitic matrix. About 70 zircon crystals were recovered through mineral separation from one eclogite sample. The zircon crystals are transparent, colourless, euhedral and stubby to elongated in shape (100–200 μm in length). In cathodoluminescence, they lack any core rim-structure, and predominantly show sector

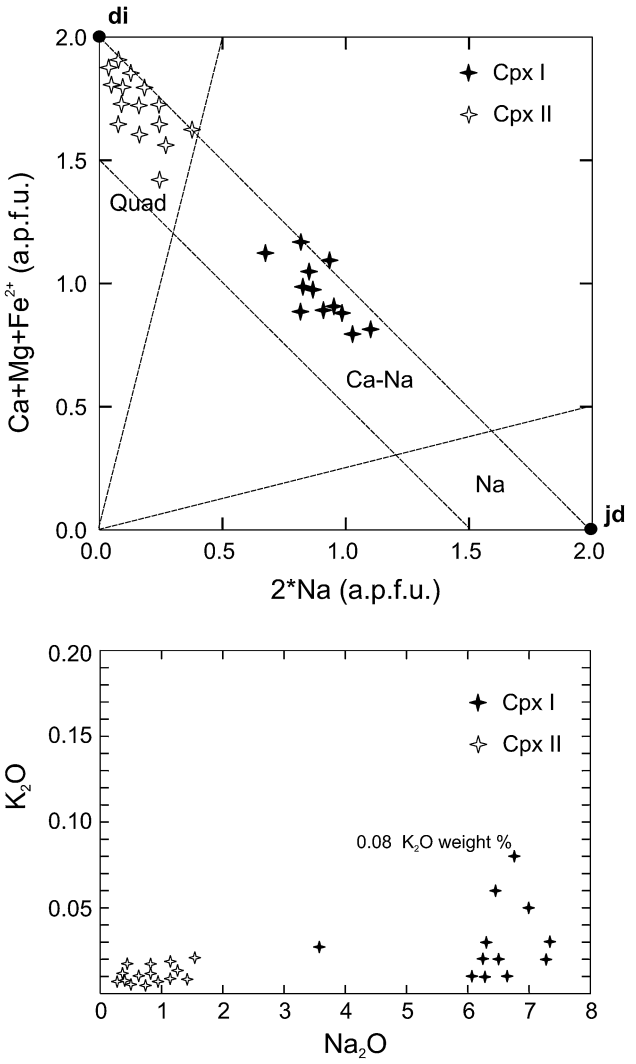

Fig. 5 **a** Classification diagram of clinopyroxene (Morimoto et al. 1988). **b** K_2O vs Na_2O wt%, eclogitic clinopyroxene (cpx_I) show a rough positive correlation with K_2O contents up to 0.08 wt%

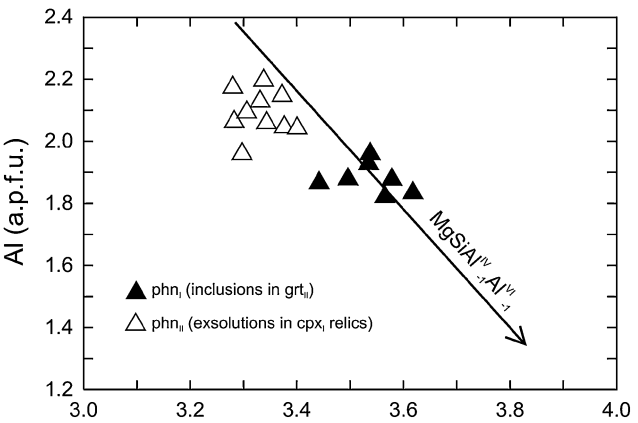

Fig. 6 Si vs Al content in phengites. The compositional variation occurs along the celadonitic substitution vector

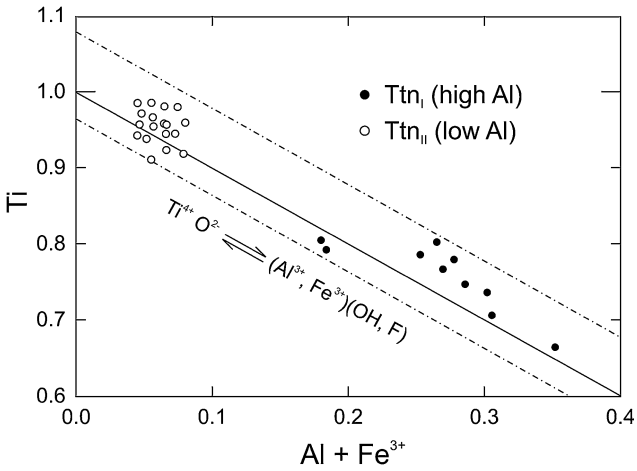

Fig. 7 Variation of Al–Fe^{3+} content in titanites. Ttn_I is stable within the eclogitic phase assemblage

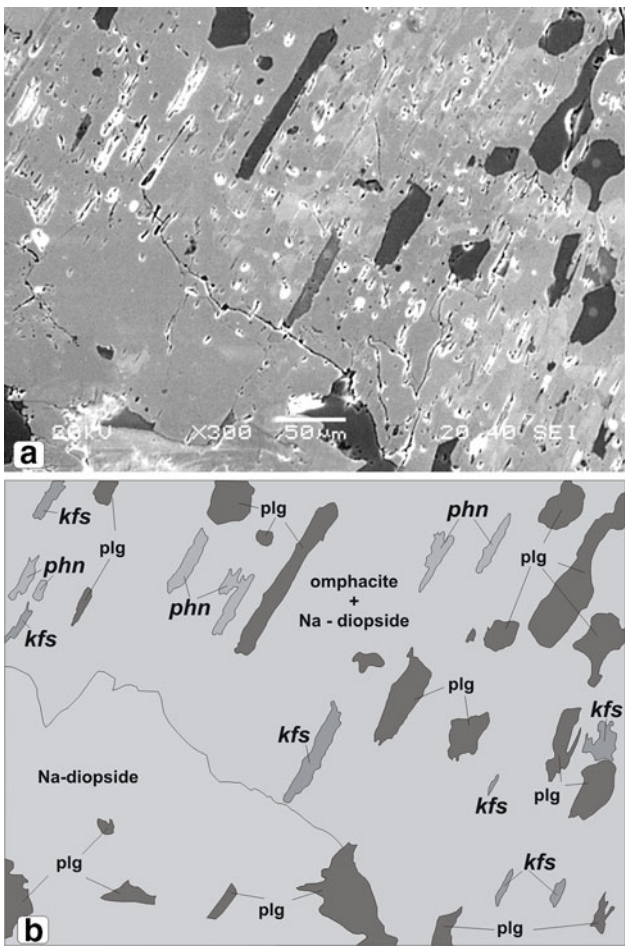

Fig. 8 **a** Back Scattered Electron images of the K-feldspar and phengite exsolutions within the omphacitic clinopyroxene relics. The exsolved lamellae are parallel to the (010) plane of the host clinopyroxene. **b** Sketch draw of Fig. 2a. K-feldspar (kfs) and phengite (phn) exsolutions are outlined together with symplectitic plagioclase (plg) resulting from the destabilization of omphacite. All mineral abbreviations are as per Kretz (1983)

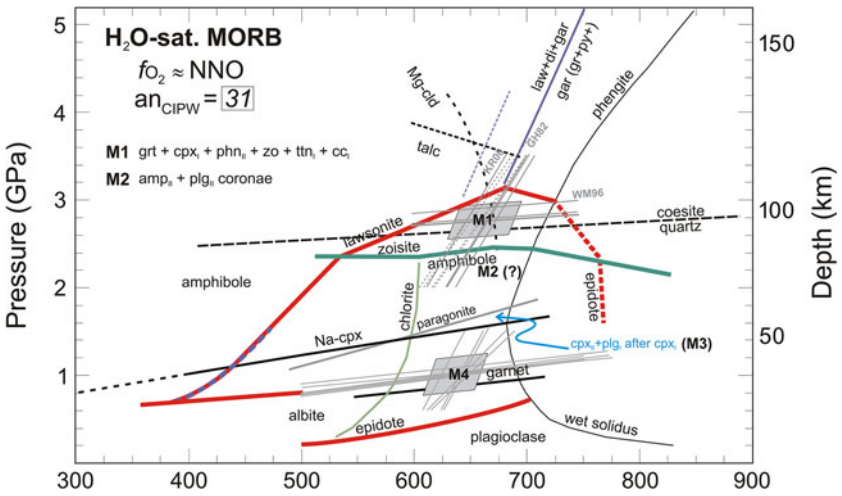

Fig. 9 Phase stabilities in hydrated MORB compositions (anCIPW = 31 %, oxygen fugacity buffered with NNO) with emphasis on epidote-bearing equilibria and amphibole stability (Poli and Schmidt 2004). P–T boxes derived for the thermobarometric estimates on the M1 eclogitic phase assemblage and the M2 amphibolitic facies phase assemblage are shown. KR00: garnet–clinopyroxene geothermometer (Krogh Ravna 2000); GH82: garnet-phengite geothermometer (Green and Helmann 1982); WM96: garnet–clinopyroxene–phengite geobarometer (Waters and Martins 1996). The M2 P–T estimates are obtained with the amphibole–plagioclase geothermometer of Holland and Blundy (1994) and the garnet–amphibole–plagioclase geobarometer of Dale et al. (2000)

zoning (Fig. 10a). SHRIMP U–Pb analysis (Table ESM7, online resource 7) measured very low U contents between 1 and 6 ppm and virtually no Th (<0.07 ppm) resulting in Th/U around 0.01. U–Pb ages were affected by large proportions of common Pb (16–60 %), due to the extremely low content in radiogenic Pb. On a Tera Wasserburg diagram 8 out of 10 analyses define a regression line with intercept at 85 ± 4 Ma. Two analyses were excluded on statistical grounds, and their inclusion in the average age would not change the value significantly (84 ± 6 Ma, MSWD 2.0 and $N = 10$). The age of 85 ± 4 Ma is considered the best estimate for the crystallization of the zircon (Fig. 10b).

The trace element analysis of 12 crystals (Table ESM8, online resource 8), including those analysed for U–Pb, confirmed low contents for all the measured elements: U and Th are in the range measured by SHRIMP (0.7–3.0 ppm and 5 ppb, respectively), P is between 10 and 15 ppm, Ti is in the order of 1–1.4 ppm, the HREE are between 10 and 100 times chondrite, and the LREE are mostly below the detection limit of a few ppb. The REE chondrite-normalized patterns show relative enrichment across the MREE (Dy/Sm = 114–157) and a flattening of the pattern for the HREE (Lu/Ho = 1.3–4.6). The Eu/Eu* [Eu/((Sm + Gd)/2)] calculated for five of the analyses indicates a negligible negative anomaly.

The zircons contain rare, submillimetric inclusions of Na–K amphibole (Table ESM9, online resource 9), but no plagioclase, suggesting that they crystallize during the earlier exhumation stages, at lower pressure than the peak assemblage (M1), but still at eclogite facies conditions.

7 Discussion and conclusions

7.1 UHP metamorphism in the Ulfas eclogites?

The Ulfas eclogites are preserved as relic boudins within garnet amphibolite bodies which display a pervasive re-equilibration at amphibolite facies conditions. In such conditions, textural aspects of the eclogitic paragenesis are difficult to assess.

With respect to other Cretaceous eclogites from the Koralpe-Wölz unit, the Ulfas eclogites differ for the absence of Ca-amphibole in the peak-pressure assemblage. Amphibole is present only within retrograde phase assemblages postdating the pressure peak, commonly as symplectitic phase together with Na-poor clinopyroxene or plagioclase. No amphibole inclusions were found within eclogitic garnet (grt_{II}) and no amphibole crystals were found in textural equilibrium with other eclogitic phases (zoisite, phengite and Na-clinopyroxene) in the matrix.

Initial decompressional stages (M2 and M3) result in the formation of Jd_{10} clinopyroxene + pargasitic amphibole symplectites. The only presence of Jd_{10} content within clinopyroxene is not sufficient to define eclogitic conditions, however, the presence of some Na within the clinopyroxene coupled with the absence of plagioclase point to, at least, high-pressure amphibolite facies conditions, close to the amphibolite/eclogite facies boundary.

As the Texel basement constitutes a polymetamorphic unit that had experienced, at least, both the Variscan and the Alpine metamorphic events, phase assemblages and

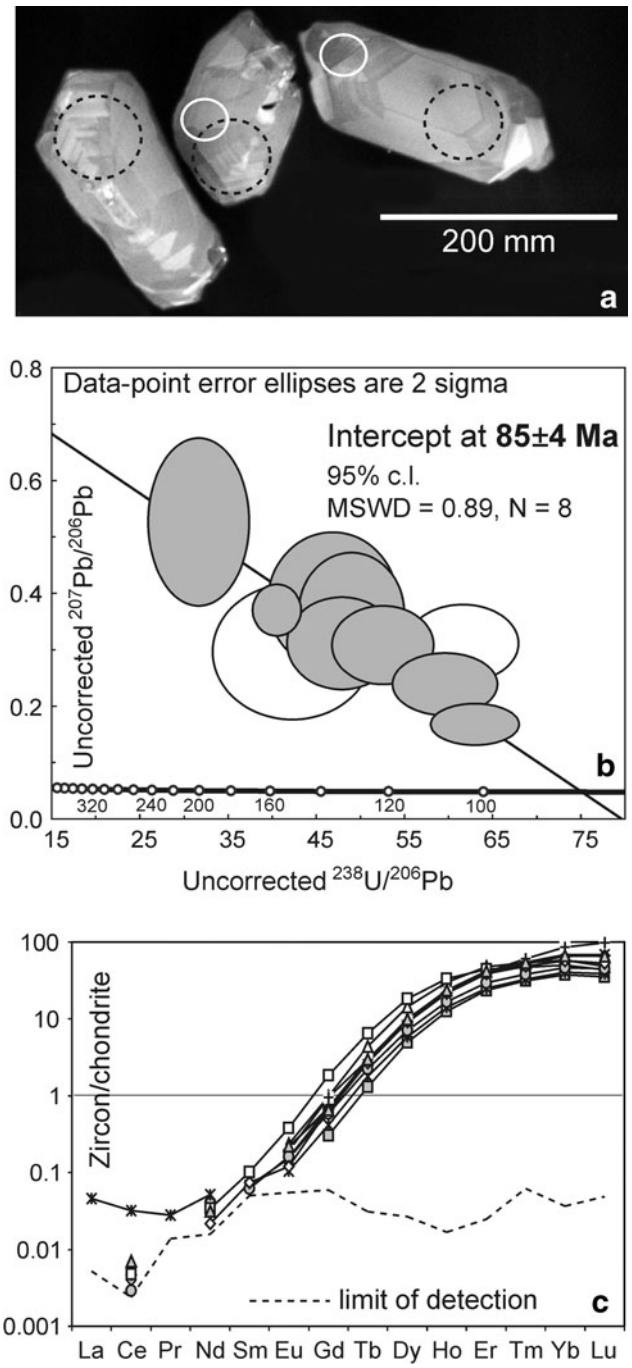

Fig. 10 Zircon zoning and composition. **a** Cathodoluminescence image of dated zircon crystals with location of the SHRIMP (*white circle*) and LA-ICPMS pits (*dashed black circle*). **b** Tera-Wasserburg diagram for uncorrected U–Pb data. The average age is defined by the intercept of the regression line forced to common Pb composition after Stacey and Kramer (1975). The two data represented by white ellipses are excluded from the regression. **c** Chondrite-normalized REE patterns of zircons. The detection limit is also plotted

mineral zoning in rocks belonging to this unit should be interpreted in the light of the complex and polyphasic tectonometamorphic evolution.

The peculiar zoning of garnet porphyroblasts could be the results of superposed orogenic events or, alternatively, record the prograde + retrograde metamorphic evolution. In our opinion, the Ca-rich garnet cores present in the Ulfas eclogites are inherited, probably from a pre-Alpine age. The presence of minute rutile inclusions in the garnet core, versus the presence of titanite in the HP assemblage, is not in line with a prograde PT path from garnet core to rim, and rather supports significantly different metamorphic conditions during garnet core formation. Similar zoning patterns of garnets from eclogites and adjacent rocks in the Saltaus Valley (Texel Complex) were reported by Habler et al. (2006), with substantially the same interpretation as proposed here. The outer garnet rims (grt_{III}) display variable composition (Fig. 4), probably as an effect of progressive breakdown of garnet to form Fe-pargasitic amphibole + plagioclase coronae around porphyroblasts. The locally higher Ca-content with respect to eclogitic grt_{II} is likely caused by not homogeneous re-equilibration of garnet in amphibole + plagioclase symplectites.

The P–T conditions for the peak-pressure assemblage have been derived from conventional geothermobarometry. The absence of kyanite in the peak-pressure mineral assemblage excludes the use of net-transfer reactions, which are less affected by the problem of estimation of Fe^{3+} in Na-clinopyroxene. The problem of the independent estimation of Fe^{3+} in eclogites minerals such as garnet and clinopyroxene is real and could affect significantly thermobarometric results. As the Fe^{3+}/Fe^{tot} was not independently determined, P–T uncertainties could be larger, especially for temperatures determined by the garnet–clinopyroxene exchange thermometer. However, our P–T estimates are supported by existing experimental phase diagrams for MORB-like systems (Poli and Schmidt 2004 and ref.incl.). In the presence of H_2O- and a Ca-bearing phase like zoisite, the amphibole-free assemblages at temperature of 550–700 °C occur at pressures between 2.4 and 3.1 GPa (Fig. 9).

Equilibrium pressures above the amphibole stability in MORB-like system are also supported by the unusually high K-content in Na-clinopyroxene and the occurrence of exsolution of K-bearing minerals. K-feldspar and phengite lamellae occur together with oligoclase patches (Fig. 8). The outlines of K-feldspar and phengite lamellae are almost straight instead of those of oligoclase patches. The shape and the iso-orientation of K-feldspar and phengite lamellae suggest that their formation post-date the crystallization of the host clinopyroxene. Even though the presence of exsolved K-phase in clinopyroxene from eclogites cannot be taken alone as a proof of former UHP conditions (e.g. Konzett et al. 2008) in the case of the Ulfas eclogites, H_2O availability as suggested by the ubiquity of zoisite should prevent K-feldspar to crystallize. It is worth

remembering that flushing and metasomatism by K-bearing aqueous fluids, as an alternative explanation, should result at high pressure in ubiquitous precipitation of phengite, not K-feldspar (Poli and Schmidt 1995; Schmidt and Poli 1998; Hermann 2002; Hermann and Spandler 2008). H_2O–CO_2 mixed fluids would not account for the occurrence of K-feldspar, because phengite is the potassium phase stable at HP even with carbonates, at pressures up to more than 9 GPa and temperatures to 900–1,000 °C, in bulk compositions from basaltic to intermediate (Schmidt and Poli 2013; Grassi and Schmidt 2011); again, phengite, and not K-feldspar, is in equilibrium on the carbonatitic solidus, when H_2O is available. Furthermore any K-addition should result in a K enrichment of the bulk composition, which is not observed in the Ulfas eclogites, where the bulk K_2O content is lower than 0.30 wt% (Table ESM6, online resource 6).

These considerations further preclude the possibility that K-feldspar could be a pristine phase overgrowth by eclogitic clinopyroxene. The similar textural aspects displayed by phengite lamellae suggest that these formed by a similar process as the K-feldspar lamellae.

White mica exsolutions within clinopyroxene were reported from UHP eclogites of the Erzgebirge Crystalline Complex (Bohemian Massif) by Schmädicke and Müller (2000). K-feldspar in clinopyroxene from UHP rocks was also reported from diopside in calcitic and dolomitic marbles (Becker and Altherr 1992; Zhang et al. 1997) and from garnet–clinopyroxene rocks of the Kokchetav Massif (Perchuk et al. 2002). In all these cases the K-rich exsolutions were interpreted as indication of the presence of former clinopyroxene with high K-content coexisting with coesite ± diamond at UHP conditions.

The oligoclase patches (in this case with clear distinct shape with respect to K-feldspar and phengite lamellae) represent, in our interpretation, the eclogite to amphibolite facies decompressional stage. During this stage omphacitic clinopyroxene was progressively transformed into diopside + amphibole + plagioclase symplectites.

Unquestionable evidences for the attainment of UHP conditions in the Ulfas eclogites such as the occurrence of coesite and/or diamond are lacking. However, several clues that the Ulfas eclogites were equilibrated within the coesite stability field are present. The relatively "high" K-content of clinopyroxene is the strongest clue for UHP metamorphism. Experimental data related to MORB-like compositional system (Schmidt and Poli 1998 and ref. incl.) suggest that the K-content of clinopyroxene coexisting with a K-phase (phengite in the pressure range of interest) increases with increasing pressure. As the whole rock composition of the Ulfas eclogite is close to experimentally investigated compositions, similar K-contents and K-contents trends are expected among experimental and natural clinopyroxenes. A comparison of chemical data of the Ulfas clinopyroxenes with experimental ones suggests that the determined K-contents (up to 0.09 K_2O wt%) are indicative of equilibrium pressure in excess of 2.5 GPa.

Incorporation of K in clinopyroxene structure could also occur at very low pressures and temperatures, below 0.5 GPa and T <400 °C, but is limited to peculiar bulk rock composition (Tsujimori and Liou 2005) with high Cr-content (up to 11 Cr_2O_3 wt%) and are associated to mineral phases that are lacking in the common mafic eclogite facies assemblages (like albite, tremolite and uvarovite, Tsujimori and Liou 2005). In those cases the incorporation of K in the clinopyroxene structure is clearly correlated with the Cr-content: Cr + K + Na increases as Ca + Fe + Mg decrease to balance cation charges. Moreover, no K-phases are present, so the K_2O that enters the clinopyroxene structure is simply controlled by the amount of K of the chemical system, which it is not the case of the Ulfas eclogites.

7.2 Interpretation of U–Pb zircon ages

Zircon crystals are characterized by low trace element contents, including Th and U, low Th/U ratio, negligible negative Eu anomaly and relatively flat HREE pattern (Fig. 10c). The low Th/U is often observed in metamorphic zircon that formed in sub-solidus conditions (Heaman et al. 1990; Rubatto and Gebauer 2000) and in the presence of a Th-rich phase, which in the eclogites could be zoisite. The very low trace elements content is also typical of metamorphic zircon, whereas magmatic zircon has, for example, HREE >100 times chondrite (e.g. Heaman et al. 1990; Hoskin and Schaltegger 2003). The small negative Eu anomaly and the flat HREE pattern suggest crystallization at HP conditions in the absence of feldspar and in the presence of garnet, respectively (e.g. Rubatto 2002). Their REE signature also excludes the possibility that the zircon formed during amphibolitization of the rock when plagioclase was forming and garnet was being consumed. The rare inclusions of Na–K amphibole within the analysed zircons suggest that they crystallized during the early decompressional stages, within the amphibole-stability field, but still in absence of plagioclase.

The low Ti contents correspond to a Ti-in-zircon T of ~600 °C using the calibration of Watson and Harrison (2005) at a Ti activity of 1. Given the presence of titanite in the HP assemblages, the activity of Ti was below unity and closer to 0.5 (Watson and Harrison, 2005) and the temperatures need to be corrected to ~650 °C. This excludes that zircons could be magmatic relicts and support crystallization close to the pressure peak.

The crystal shape and the sector zoning of the dated zircon are similar to what has been documented for zircon

formed in metamorphic veins such as the Monviso HP vein (Rubatto and Hermann 2003). The likely presence of interstitial fluids (no veining is observed) in the rock at the time of zircon formation is expected to favour chemical equilibrium between the phases.

Following these considerations, the obtained U–Pb age of 85 ± 4 Ma should be considered as the minimum, but close to the age for HP metamorphism recorded in the Ulfas eclogites.

Early garnet growth at 95–94 Ma and ceasing garnet formation at 90−88 ± 5 Ma was envisaged for the other eclogites of the Koralpe-Wölz unit (Habler et al. 2006; Thöni et al. 2008). Considering that most of the Köralpe-Wölz eclogites are amphibole-bearing, our dataset well agrees with existing data.

7.3 Geodynamic significance of the Ulfas eclogites

The suggested peak pressures for the Ulfas eclogites are at least close to the quartz–coesite transition, clearly exceeding previous estimates ranging between 1.0 and 1.4 GPa (Hoinkes et al. 1991; Habler et al. 2006) for the Cretaceous eclogite facies metamorphism of the Texel Complex. As thermobarometric estimates are based on post-exsolution clinopyroxene compositions, the possibility that calculated pressure is "minimum pressures", should be taken into account, suggesting that the Ulfas eclogites may have been exhumed from even greater depth.

The timing and equilibrium conditions obtained for the Ulfas eclogites are close to other HP units of the Austroalpine of the Eastern Alps, such as the Koralpe-Saualpe eclogitic complex (2–2.4 GPa, around 90 Ma; Miller et al. 2005a; Thöni 2006 and ref. incl.) and he Pohorje unit ($P > 2.1$ GPa at 90 Ma; Janák et al. 2004; Sassi et al. 2004; Miller et al. 2005b; Thöni et al. 2008). Our new data on the Ulfas eclogites highlight the similarities among all the Cretaceous HP units (the "Koralpe-Wölz unit" of Schimd et al. 2004; Froitzheim et al. 2008; Handy et al. 2010) of the Eastern Alps. They also point to the existence of several sector of Africa-Adria derived continental crust that have been subducted to ≥80 km and then exhumed to shallow crustal levels between 90 and 70 Ma.

The fact that our HP age and the cooling ages measured by Thöni et al. (2008) overlap is expected given the relatively large analytical errors and the fast nature of eclogite exhumation. The peak-pressure assemblages of the Saualpe eclogites are dated from 94 ± 1 Ma (G1 stage in Fig. 11) to 91–90 Ma (G2 stage in Fig. 11, Thöni et al. 2008). Similar to the metapelites and the other eclogites of the Texel Complex, also the Saualpe rocks display a clockwise exhumation path (Fig. 11), characterized by re-equilibration at amphibolite facies conditions (G3 in Fig. 11). Geochronological data for the Koralpe-Wölz unit eclogites to the east of Tauern Window suggest a short-lived high-P event, that lasted <10 Ma (Miller et al. 2005a, b; Thöni et al. 2008), followed by fast exhumation that brought the eclogites at shallow crustal levels before 75–70 Ma (Wiesinger et al. 2006; Thöni et al. 2008). An almost identical evolution could be envisaged for the Texel Complex, where 77–75 Ma greenschist mylonites mark the contact between the Texel and the Schneeberg Complex (Sölva et al. 2005).

The occurrence of a subduction zone in the Eastern Alps during the Cretaceous, along which large portions of the Austroalpine upper lithosphere were dragged to depth, has been suggested and discussed by several authors (e.g. Thöni and Jagoutz 1993; Janák et al. 2004; Schimd et al. 2004; Sölva et al. 2005; Miller et al. 2005b; Thöni 2006; Thöni et al. 2008) and it is widely accepted. The new data on the Ulfas eclogites reinforce the interpretation that more

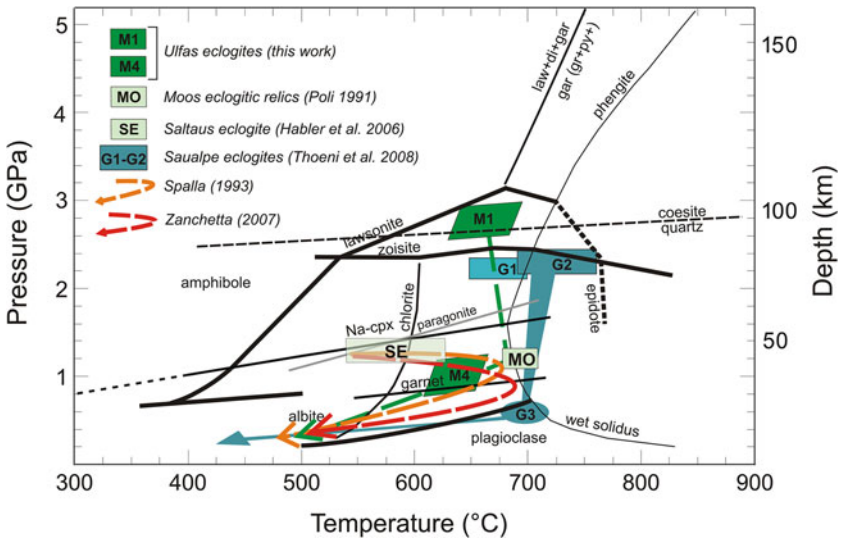

Fig. 11 P–T path of the Ulfas eclogites compared with the Saualpe eclogites (Thöni et al. 2008) and other eclogites from the Texel Complex (Poli 1991; Habler et al. 2006). P–T paths obtained from the metapelites of the Texel Complex (Spalla 1993; Zanchetta 2007) are also shown

than one Cretaceous eclogitic units of the Eastern Alps were simultaneously subducted to more than 2 GPa in a short time span between 95 and 85 Ma.

The Cretaceous high-pressure metamorphism of the Austroalpine Koralpe-Wölz unit is interpreted in the frame of the Eoalpine orogeny (Thöni and Jagoutz 1993) that resulted from the closure of a branch of the Neotethys (Meliata–Maliac ocean, Thöni and Jagoutz 1993; Schmid et al. 2008; Handy et al. 2010). The closure of the Meliata ocean led to the convergence of a supposed Austroalpine microplate (Alcapia microplate in Handy et al. 2010) located to the N of the Meliata ocean, with the Africa-Adria margin. The resulting collision caused S- to SE-directed subduction of the Alcapia continental crust, high-pressure metamorphism, and later exhumation of eclogites, now exposed in the Koralpe-Wölz unit (e.g. Sölva et al. 2005).

The extension of the Meliata Ocean in the Eastern Alps region is highly debatable as no ophiolitic remnants are preserved to the north or south of the Cretaceous high-pressure belt and the closest oceanic units unambiguously attributed to the Meliata domain occur far to the SE, in the internal Dinarides (Pamic 2002). The Neotethyan oceanic branches, now preserved in the Carpathian–Dinaridic orogenic system, closed by the end of the Jurassic (Bortolotti et al. 2005; Dal Piaz et al. 1995), several tens of million years before the mid-Cretaceous subduction of the Austroalpine units.

In the same palaeotectonic frame, another hypothesis considers intracontinental initiation of subduction within the Austroalpine domain (Janák et al. 2004, 2006; Stüwe and Schuster 2010). Subduction initiation was triggered by the gravitational instability of the mantle lithosphere that was previously thickened during the Permian and Triassic thermal events (Schuster and Stüwe 2008). Intracontinental subduction that was not preceded by ocean subduction has been rarely documented in the geological record (e.g. Faure et al. 2009).

An alternative geodynamic scenario (Zanchetta et al. (2012) considers the HP units of the Eastern Alps to be related to the pre-collisional phase of the Alpine orogenesis, as already proposed for the Sesia eclogites in the Western Alps (Dal Piaz et al. 1972; Compagnoni et al. 1977; Polino et al. 1990). It has been suggested (Zanchetta et al. 2012) that subduction nucleated in the Africa-Adria margin, which was previously attenuated during the Permian to Jurassic rifting. Recent U–Pb geochronology indicates that the first cycle of HP metamorphism in the Western Alps, Sesia Zone, occurred already at $\sim$80 Ma, and was then followed by a second cycle at 70–60 Ma (yo–yo subduction; Rubatto et al. 2011). This first HP stage in the Western Alps brings the age of subduction in the West and East Alpine chain much closer in time.

A striking feature of the Cretaceous Asutroalpine HP units, from the Sesia Zone in the west to the Pohorje in the east is the coexistence of HT/LP relics of Permian to Triassic age overprinted by the Cretaceous high-pressure metamorphism (Schuster and Stüwe 2008; Zanchetta et al. 2012). Recent data (Tumiati et al. in preparation) indicate that also the Texel Complex shares this feature with the other Koralpe-Wölz units.

All this data suggest that Cretaceous HP metamorphism interested only crustal portions of the Austroalpine margin that were previously involved in the Permian and Triassic thermal events (Dal Piaz and Martin 1998; Marotta et al. 2009). In this scenario the Cretaceous subduction nucleated within the attenuated northern Africa-Adria margin, favoured by the latest Albian/Cenomanian onset of convergence between Africa-Adria-Arabia and Eurasia (Dercourt et al. 2000). The distal Austroalpine margin, densified by magmatic underplating and gabbro intrusions during the Permian to Jurassic rifting, was swallowed first in the Cretaceous subduction zone, giving rise to pre-collisional HP metamorphism (Zanchetta et al. 2012). The present day SAM fault network (Hoinkes et al. 1999) could be tentatively interpreted as remnants of a precursor of orogen-scale importance that played a significant role in the exhumation of the HP units within the Cretaceous orogenic wedge.

Acknowledgments The Electron Microscopy Unit at the ANU is thanked for access to the SEM for CL imaging. The careful reviews by two anonymous reviewers and G.V. Dal Piaz helped us to improve the quality of the paper. We warmly thank F·P. Sassi and G.V. Dal Piaz for editorial handling. An earlier version of the paper benefited also of suggestions from M. M. Thöni and two anonymous reviewers. This work benefited from the financial support of the CARG project (directed by Volkmar Mair) of the Autonome Provinz Bozen.

References

Bargossi GM, Bove G, Cucato M, Gregnanin A, Morelli C, Moretti A, Poli S, Zanchetta S, Zanchi A (2010) Note Illustrative della Carta Geologica d'Italia alla scala 1:50.000, F. 013 MERANO. ISPRA: Servizio Geologico d'Italia. Provincia Autonoma di Bolzano, Alto Adige

Becker H, Altherr R (1992) Evidence form ultra-high-pressure marbles for recycling of sediments into the mantle. Nature 358(27):745–748

Black LP, Kamo SL, Allen CM, Aleinikoff JN, Davis DW, Korsch RJ, Foudoulis C (2003) TEMORA 1: a new zircon standard for Phanerozoic U–Pb geochronology. Chem Geol 200:155–170

Bortolotti V, Marroni M, Pandolfi L, Principi G (2005) Mesozoic to tertiary history of the Mirdita ophiolites, Northern Albania. Isl Arc 14:471–493

Chopin C (1984) Coesite and pure pyrope in high-grade blueschists of the Western Alps: a first record and some consequences. Contrib Miner Petrol 86:107–118

Chopin C (2003) Ultrahigh-pressure metamorphism: tracing continental crust into the mantle. Earth Planet Sci Lett 212:1–14

Coleman RG, Lee DE, Beatty LB, Brannock WW (1965) Eclogites and eclogites: their differences and similarities. Geol Soc Am Bul 76:483–508

Compagnoni R, Dal Piaz GV, Hunziker JC, Gosso G, Lombardo B, Williams PF (1977) The Sesia–Lanzo zone, a slice of continental crust with alpine high pressure-low temperature assemblages in the Western Italian Alps. Rend Soc It Min Petr 33:281–334

Dal Piaz GV, Martin S (1998) Evoluzione litosferica e magmatismo nel dominio Austro-Sudalpino dall'orogenesi Varisica al rifting Mesozoico. Mem Soc Geol It 53:43-62

Dal Piaz GV, Hunziker JC, Martinotti G (1972) La Zona Sesia–Lanzo e l'evoluzione tettonico-metamorfica delle Alpi nordoccidentali interne. Mem Soc Geol It 11:433–466

Dal Piaz GV, Martin S, Villa I, Gosso G, Marschalko R (1995) Late Jurassic blueschist facies pebbles from the Western Carpathian orogenic wedge and paleostructural implications for Western Tethys evolution. Tectonics 14:874–885

Dale J, Holland T, Powell R (2000) Hornblende-garnet-plagioclase thermobarometry: a natural assemblage calibration of the thermodynamics of hornblende. Contrib Miner Petrol 140:353–362

Dercourt J, Gaetani M, Vrielynck B, Barrier E, Biju-Duval B, Brunet MF, Cadet JP, Crasquin S, Sandulescu M (2000) Atla Peri-Thetys Paleogeographical Maps. I-XX. CCGM/CGMW, Paris, pp. 269, 24 maps and explanatory notes

Eggins SM, Rudnick RL, McDonough WF (1998) The composition of peridotites and their minerals: a laser ablation ICP-MS study. Earth Planet Sci Lett 154:53–71

Faure M, Shu L, Wang B, Charvet J, Choulet F, Monie P (2009) Intracontinental subduction: a possible mechanism for the early Paleozoic Orogen of SE China. Terra Nova 21:360–368

Froitzheim N, Plasienka D, Schuster R (2008) Alpine tectonics of the Alps and Western Carpathians. In: McCann T (ed) Mesozoic and Cenozoic: the geology of Central Europe, vol 2. Geological Society, London, pp 1141–1232

Grassi D, Schmidt MW (2011) The melting of carbonated Pelites from 70 to 700 km depth. J Petrol 52:765–789

Green TH, Helmann PL (1982) Fe-Mg partitioning between coexisting garnet and phengite at high pressure, and comments on a garnet-phengite geothermometer. Lithos 17:253–266

Handy M, Schmid S, Bousquet R, Kissling E, Bernoulli D (2010) Reconciling plate-tectonic reconstructions of Alpine Tethys with the geological–geophysical record of spreading and subduction in the Alps. Earth-Sci Rev 102:121–158

Habler G, Thöni M, Sölva H (2006) Tracing the high pressure stage in the polymetamorphic Texel Complex (Austroalpine basement unit, Eastern Alps): P-T-t-d constraints. Miner Petrol 88: 269–296

Heaman LM, Bowins R, Crocket J (1990) The chemical composition of igneous zircon suites—implications for geochemical tracer studies. Geochim Cosmochim Acta 54:1597–1607

Heinrich CA (1986) Eclogite facies regional metamorphism of hydrous mafic rocks in the central alpine Adula nappe, Central Alps. J Petrol 27:23–154

Hermann J (2002) Experimental constraints on phase relations in subduction continental crust. Contrib Miner Petrol 143:219–235

Hermann J, Spandler CJ (2008) Sediments at sub-arc depths: an experimental study. J Petrol 49:717–740

Hoinkes G, Kostner A, Thöni M (1991) Petrologic constraints for eoalpine eclogite facies metamorphism in the Austroalpine Oetztal basement. Miner Petrol 43:237–254

Hoinkes G, Koller F, Rantitsch G, Dachs E, Höck V, Neubauer F, Schuster R (1999) Alpine metamorphism of the Eastern Alps. Schweiz Miner Petrogr Mitt 79:155–181

Holland TJB, Blundy JD (1994) Non-ideal interactions in calcic amphiboles and their bearing on amphibole-plagioclase thermometry. Contrib Miner Petrol 116:433–447

Hoskin PWO, Schaltegger U (2003) The composition of zircon and igneous and metamorphic petrogenesis. Rev Miner Geochem 53:27–62

Janák M, Froitzheim N, Lupták B, Vrabec M, Krogh Ravna EJ (2004) First evidence for ultrahigh-pressure metamorphism of eclogites in Pohorje, Slovenia: tracing deep continental subduction in the Eastern Alps. Tectonics 23, TC5014. doi:10.1029/2004TC001641

Janák M, Froitzheim N, Vrabec M, Krogh Ravna EJ, De Hoog JCM (2006) Ultrahigh-pressure metamorphism and exhumation of garnet peridotites in Pohorje, Eastern Alps. J Metamor Geol 24:19–31

Konzett J, Frost DJ, Proyer A, Ulmer P (2008) The Ca-Eskola component in eclogitic clinopyroxene as a function of pressure, temperature and bulk composition: an experimental study to 15 GPa with possible implications for the formation of oriented SiO_2-inclusions in omphacite. Contrib Mineral Petrol 155: 215–228

Kretz R (1983) Symbols for rock-forming minerals. Am Mineral 78:277–279

Krogh Ravna EJ (2000) The garnet-clinopyroxene Fe–Mg geothermometer: an updated calibration. J Metamor Geol 18:211–219

Krogh Ravna EJ, Terry MP (2004) Geothermobarometry of UHP and HP eclogites and Schists, an evaluation of equilibria among garnet-clinopyroxene-kyanite-phengite-coesite/quartz. J Metamor Geol 22:579–592

Ludwig KR (2000) Isoplot/Ex version 2.4. A geochronological toolkit for Microsoft Excel. Berkeley Geochronological Centre Spec Pub, Berkeley

Marotta A, Spalla M, Gosso G (2009) Upper and lower crustal evolution during lithospheric extension: numericla modelling and natural footprints from the European Alps. Spec Pub Geol Soc Lond 312:33–72

Morimoto N, Fabries J, Ferguson AK, Ginzburg IV, Ross M, Seifert FA, Zussman J, Aoki K, Gottardi G (1988) Nomenclature of pyroxenes. Am Mineral 73:1123–1133

Miller C, Thöni M, Konzett J, Kurz W, Schuster R (2005a) Eclogites form the Koralpe and Saualpe type-localities, Eastern Alps, Austria. Mitt Österr Miner Ges 150:227–263

Miller C, Konzett J (2005b) Comment on "First evidence for ultrahigh-pressure metamorphism of eclogites in Pohorje, Slovenia: tracing deep continental subduction in the Eastern Alps" by Marian Janák et al. Tectonics 24. doi:10.1029/2004TC001765

Miller C, Mundil R, Thöni M, Konzett J (2005c) Refining the timing of eclogite facies metamorphism: a geochemical, petrological, Sm–Nd and U–Pb case study from the Pohorje Mountain, Slovenia (Eastern Alps). Contrib Miner Petrol 150:70–84

Pamic J (2002) The Sava-Vardar Zone of the Dinarides and Hellenides versus the Vardar ocean. Eclogae Geol Helv 95: 99–113

Perchuk LL, Safonov OG, Yapaskurt VO, Barton JM (2002) Crystal-melt equilibria involving potassium-bearing clinopyroxene as indicator of mantle-derived ultrahigh-potassic liquids: an analytical review. Lithos 60:89–111

Poli S (1991) Reaction spaces and P–T paths: from the amphibole eclogite to the greenschist facies in the Austroalpine domain (Oetztal Complex). Contrib Miner Petrol 106:399–416

Poli S, Schmidt MW (1995) Water transport and release in subduction zones: experimental constraints on basaltic and andesitic systems. J Geophys Res 100:22299–22314

Poli S, Schmidt MW (2004) Experimental Subsolidus studies on Epidote minerals. In: Liebscher A, Franz G (eds) Epidotes, Rev Mineral Geochem 56: 171–192

Polino R, Dal Piaz GV, Gosso G (1990) Tectonic erosion at the Adria margin and accretionary processes for the Cretaceous orogeny of the Alps. Mem Soc Geol France 156:345–367

Reinecke T (1991) Very high-pressure metamorphism and uplift of coesite-bearing metasediments from the Zermatt-Saas zone, Western Alps. Eur J Miner 3:7–17

Rubatto D (2002) Zircon trace element geochemistry: partitioning with garnet and the link between U–Pb ages and metamorphism. Chem Geol 184:123–138

Rubatto D, Gebauer D (2000) Use of cathodoluminescence for U–Pb zircon dating by ion microprobe: some examples from the Western Alps. In: Pagel M, Barbin V, Blanc P, Ohnenstetter D (eds) Cathodoluminescence in Geosciences. Springer, Heidelberg, pp 373–400

Rubatto D, Hermann J (2003) Zircon formation during fluid circulation in eclogites (Monviso Western Alps): implications for Zr and Hf budget in subduction zones. Geochim Cosmochim Acta 67:2173–2187

Rubatto D, Regis D, Hermann J, Boston K, Engi M, Beltrando M, McAlpine SRB (2011) Yo–Yo subduction recorded by accessory minerals in the Sesia Zone, Western Alps. Nat Geosci 4:338–342

Sassi R, Mazzolli C, Miller C, Konzett J (2004) Geochemistry and metamorphic evolution of the Pohorje Mountain eclogites from the easternmost Austroalpine basement of the Eastern Alps (Northern Slovenia). Lithos 78:235–261

Schmädicke E, Müller WF (2000) Unusual exsolution phenomena in omphacite and partial replacement of phengite by phlogopite + kyanite in a eclogite from the Erzgebirge. Contrib Miner Petrol 139:629–642

Schmid SM, Haas R (1989) Transition from near-surface thrusting to intrabasement decollement, Schlinig thrust, Eastern Alps. Tectonics 8:697–718

Schmid SM, Fügenschuh B, Kissling E, Schuster R (2004) Tectonic map and overall architecture of the Alpine orogen. Eclogae Geol Helv 97:93–117

Schmid SM, Bernoulli D, Fügenschuh B, Matenco L, Schefer S, Schuster R, Tischler M, Ustaszewski K (2008) The Alpine–Carpathian–Dinaridic orogenic system: correlation and evolution of tectonic units. Swiss J Geosci 101:139–183

Schmidt MW, Poli S (1998) Experimentally based water budgets for dehydrating slabs and consequences for arc magma generation. Earth Planet Sci Lett 163:361–379

Schmidt MW, Poli S (2013) Devolatilization during subduction. In: Rudnick RL (ed) The crust treatise on geochemistry, vol 3. Elsevier-Pergamon, Oxford (2nd edn, Holland HD, Turekian KK (eds)

Schuster R, Stüwe K (2008) Permian metamorphic event in the Alps. Geology 36:603–606

Sölva H, Grasemann B, Thöni M, Thiede R, Habler G (2005) The Schneeberg normal fault zone: normal faulting associated with Cretaceous SE-directed extrusion in the Eastern Alps (Italy/Austria). Tectonophysics 410:143–166

Spalla MI (1993) Microstructural control on the P–T path construction in metapelites of the Austroalpine crust (Texel Gruppe, Eastern Alps). Schweiz Miner Petrogr Mitt 81:197–212

Spiess R (1995) The Passeier-Jaufen line: a tectonic boundary between Variscan and eo-Alpine Meran–Mauls basement. Schweiz Miner Petrogr Mitt 75:413–425

Stacey JS, Kramers JD (1975) Approximation of terrestrial lead evolution by a two-stage model. Earth Planet Sci Lett 26:207–221

Stüwe K, Schuster R (2010) Initiation of subduction in the Alps: continent or ocean? Geology 38:175–178. doi:101130/G30528.1

Thöni M (2006) Dating the eclogite-facies metamorphism in the Eastern Alps—approaches, results, interpretations: a review. Miner Petrol 88:123–148

Thöni M, Jagoutz E (1993) Isotopic constraints for the eo-Alpine high-P metamorphism in the Austroalpine nappes of the Eastern Alps: bearing on Alpine orogenesis. Schweiz Miner Petrogr Mitt 73:177–189

Thöni M, Miller C, Blichert-Toft J, Whitehouse MJ, Konzett J, Zanetti A (2008) Timing of high-pressure metamorphism and exhumation of the eclogite-type locality (Klupperbrunn-Prickler Halt, south-eastern Austria): constraints from the correlation of the Sm-Nd, Lu-Hf, U-Pb and Rb-Sr isotopic systems. J Metamorphic Geol 26:561–581

Tsujimori T, Liou JG (2005) Low-pressure and low-temperature K-bearing kosmochloric diopside from the Osayama serpentinite melange, SW Japan. Am Mineral 90:1629–1635

Viola G, Mancktelow NS, Seward D (2001) Late Oligocene–Neogene evolution of Europe–Adria collision: new structural and geochronological evidence from the Giudicarie fault system (Italian Eastern Alps). Tectonics 20:999–1020

Waters DJ, Martins HN (1996) The Grt-Cpx-Phengite barometer. Recommended calibration and calculation method. Updated 1 Mar 1996. http://www.earth.ox.ac.uk/∼davewa/research/eclogites

Watson EB, Harrison TM (2005) Zircon thermometer reveals minimum melting conditions on earliest Earth. Science 308:841–844

Wiesinger M, Neubauer F, Handler R (2006) Exhumation of the Saualpe eclogitic unit, Eastern Alps: constraints from $^{40}Ar/^{39}Ar$ ages and structural investigations. Miner Petrol 88:149–180

Williams I (1998) U–Th–Pb geochronology by ion microprobe. In: McKibben MA, Shanks III WC, Ridley WI (eds), Application of microanalytical techniques to understanding mineralizing processes. Rev Econom Geol, pp 1–35

Zanchetta S (2006) Tectonometamorphic evolution of the Austroalpine basement in the Eastern Alps: insights from structural 3D modelling, metamorphic petrology and experimental modelling. PhD Thesis, University of Milano, 132

Zanchetta S (2007) Evoluzione tettonometamorfica delle unità di Texel e dello Schneeberg (Alpi centro-orientali). Rend Soc Geol It 4:312–314

Zanchetta S (2010) The Texel-Schneeberg boundary in the Pfossen valley (Merano, NE Italy): geological-structural map and explanatory notes. Italy J Geosci 129:395–407

Zanchetta S, Garzanti E, Doglioni C, Zanchi A (2012) The Alps in the Cretaceous: a doubly vergent pre-collisional orogeny. Terra Nova 24:351–356

Zhang RJ, Liou JG, Ernst WG, Coleman RG, Sobolev NV, Shatsky VS (1997) Metamorphic evolution of diamond bearing and associated rocks from the Kokchetav Massif, Northern Kazakhstan. J Metamor Geol 15:479–496